European Journal of Integrative Medicine 42 (2021) 101291

Contents lists available at ScienceDirect

European Journal of Integrative Medicine

journal homepage: www.elsevier.com/locate/eujim

Research paper

Inula viscosa (L.) Greuter, phytochemical composition, antioxidant, total phenolic content, total flavonoids content and neuroprotective effects

Mohammad Qneibi[a,*], Michel Hanania[b,**], Nidal Jaradat[c], Nour Emwas[a], Sireen Radwan[b]

[a] Department of Biomedical Sciences, Faculty of Medicine and Health Sciences, An-Najah National University, Nablus, Palestine
[b] Department of Chemistry, Faculty of Science, Bethlehem University, P.O. Box 9, Bethlehem, Palestine
[c] Department of Pharmacy, Faculty of Medicine and Health Sciences, An-Najah National University, Nablus, Palestine

ARTICLE INFO

Keywords:
Inula viscosa
Neuroprotective effect
Pharmacological properties
AMPA receptors
Gating properties

ABSTRACT

Introduction: Inula viscosa (L.) Greuter (DV) has been utilized in folk medicine due to its anti-inflammatory, diuretic, antiseptic, and antiphlogistic properties. Numerous studies highlighted the beneficial impact of (DV) on different diseases, yet research lacks information on its effect on neurodegeneration, specifically concerning neurotoxicity.

Methods: The EO chemical composition of (DV) hydroethanolic extract was investigated using GC–MS, while the antioxidant potential was performed using (DPPH) assay and FRAP. Total phenolic content (TPC) and total flavonoid content (TFC) were measured using Folin-Ciocalteu and aluminum chloride methods. Experiments targeted the fastest ligand-gated ion channels involved in excitotoxicity. Hence, (DV) was examined for any inhibitory actions against all AMPARs presented in the CNS via whole-cell patch-clamp electrophysiology on HEK293 cells. Moreover, the effect of (DV) on other AMPAR biophysical parameters such as desensitization and deactivation was assessed.

Results: GC–MS revealed the presence of twenty-one components, representing 100% of the total constituents. The major components were patchulane, 3-b-phenoxy-24-nor-cholan-5,20(22)-diene, 3-ethyl-3-hydroxy-5alpha-androstan-17-one and γ-gurjunene. (DV) showed strong antioxidant activity with an IC50 value (13.5 ± 0.44 μg/ml) compared to Trolox (3.23±0.92 μg/ml). High value for TPC (193.07±9.1 mg Gallic acid eq./g) and TFC (594.9 ± 12.2 mg Rutin eq./g) were found. Of the examined AMPARs, (DV) inhibited GluA1 and GluA2 homomer AMPARs but not GluA3 or GluA4. (DV) inhibited both heterologous expression forms; GluA1/2 and GluA2/3 yet showed considerable significance for GluA1/2. (DV) was also selective to particular AMPAR subunits on the desensitization and deactivation.

Conclusions: The current study showed high antioxidant potential, high total phenolics, and flavonoids and demonstrated neuroprotective properties of (DV) concerning neurotoxicity.

1. Introduction

Inula viscosa (L.) Greuter (DV) is a popular plant of Mediterranean origin used in traditional medicine. Commonly referred to as *Inula*, the herbaceous perennial plant belongs to the Asteraceae family, characterized by having sticky leaves with yellow flowers [1,2]. Various studies have researched the numerous beneficial properties of (DV), specifically antimicrobial, antipyretic, and anti-numerous inflammatory traits [3]. Additionally, many studies identified different biologically active compounds in (DV), i.e., flavonol derivatives and phytochemicals such as polyphenols and sesquiterpenes [4]. These compounds have been extracted and used in different studies to highlight the potential of this plant in cancer treatment and oxidative stress-related diseases [5]. Moreover, it is used in Morocco, Jordan, Palestine and other coastal Mediterranean countries as an anti-inflammatory, diuretic, antiseptic, antiphlogistic and hemostatic herb [6,7]. Furthermore, (DV) is used in treating diabetes mellitus, hypertension, and skin irritation caused by allergies [4,8]. However, neurological studies on the plant are scarce to evaluate the potential neuroprotective properties of (DV) towards neurodegenerative and neuropsychiatric diseases. Thus, we examined the potential of this plant to act as a neuroprotective candidate against neurotoxicity caused by excessive glutamate concentration, which has been associated with various diseases [9,10]. Specifically, the effect of (DV)

* Corresponding authors: P.O. Box 7, Nablus, Palestine.
** Corresponding authors: 5 Rue des Frères Bethlehem, Palestine.
E-mail addresses: mqneibi@najah.edu (M. Qneibi), mhanania@bethlehem.edu (M. Hanania).

https://doi.org/10.1016/j.eujim.2021.101291
Received 12 October 2020; Received in revised form 15 January 2021; Accepted 16 January 2021
1876-3820/© 2021 Elsevier GmbH. All rights reserved.

on the α-amino-3-hydroxy-5-methyl-4-isoxazolepropionic acid receptor (AMPAR). AMPARs are known to be the fastest type from the ionotropic glutamate receptors (iGluRs) family and are responsible for most of the fast-excitatory neurotransmission in CNS [11].

Epilepsy, ischemia, Amyotrophic lateral sclerosis (ALS), and Alzheimer's disease (AD) are a few of the diseases implicated with glutamate-induced excitotoxicity [12,13]. Some research has explored the possible mechanism of neuronal death; an increasing body of evidence suggests the progression and pathogenesis of these diseases are associated with excitotoxicity [14]. The receptors accountable for the majority of the excitatory neurotransmission and are responsive to glutamate are AMPARs, which are generally expressed on the post-synaptic neuron [15]. Excessive activation of AMPARs can provoke neurodegeneration by activating the calcium-dependent enzymatic pathways [10]. In the pursuit of acquiring treatment for various chronic neurodegenerative diseases, recent articles investigate the options of potential AMAPR antagonists to reduce excitotoxicity [16,17]. Subsequent work on global ischemia in animal models demonstrated that AMPAR antagonists were more effective in the prevention of neuronal loss than NMDAR [18]. Nevertheless, symptoms of extrapyramidal, dependence, tolerance, and respiratory depression are often the results coinciding with many of the researched antagonists during the clinical trial phase [19]. The assembly of AMPARs involves four core subunits (GluA1–4) that can be arranged in a homomeric or heterogenic form. Importantly, the component subunits determine the function, trafficking, and ion permeability of AMPARS and require glutamate alone for channel activation [11]. The most abundant forms of AMPARs are the heterogeneous GluA1/A2 and GluA2/3, which are mainly expressed in the mature hippocampus [14,15]. Different AMPAR subunits are affiliated with diverse neurological diseases due to holding different ion permeability and functions [16,17]. For example, GluA2 receptors are accountable for calcium impermeability and a low percentage of their expression is associated with ALS [20]. On the contrary, GluA2 lacking AMPARs subunits provide a stronger voltage due to the increased ion influx, and dysregulation in their expression is associated with various diseases [21].

Thus, the effect of (DV) was tested individually on all homomeric AMPAR subunits; GluA1, GluA2, GluA3, and GluA4, and the most abundant heterologous AMPARs in the CNS; which are GluA1/2 and GluA2/3. In an attempt to increase the efficacy and safety of possible AMPAR antagonists, we investigated the potential natural (DV) for antioxidative and neuroprotective properties via inhibition of AMPARs and the minimization of other biophysical gating properties.

2. Materials and methods

2.1. Preparation and extraction of (DV)

The leaves of the (DV) plant were gathered in July of 2019 from Al-Khader town, the western region of Bethlehem-Palestine (Coordinates: 31°41′34″N 35°09′59″E). Leaves were dried for two weeks at ordinary temperature and then powdered coarsely. The plant was morphologically identified as *Inula viscosa* by Botanist Dr. Omar Darissa. The plant population was examined in their natural habitat in Bethlehem district as well as in the Plant Biotechnology Research Center at Bethlehem University-Palestine. They have erect and glandular stems that are 50–120 cm high. The leaves are sessile, linear triangular with serrulate margins and subacute apices. Achenes are short, cylindrical and abruptly contracted below the pappus. The pappus has dense hairs about 6–8 mm long and is connate at their base. The plant sample was kept under the voucher specimen code of Pharm-PCT-862. The EO of the DV plant was isolated using the microwave-ultrasonic method as described by Jaradat et al., with minor modifications [22]. Within the isolation process, the powder suspension was exposed to ultrasonic- and microwaves to improve the extraction process. A 1 L round-bottom flask containing 100 g of the dried plant powder was placed in microwave-ultrasonic apparatus. In this flask, the powder was mixed in 500 ml distilled water. Then, the flask was connected with the Clevenger apparatus which was placed in the same apparatus. During the isolation process, the power of the microwave extractor apparatus was adjusted at 1000 W. The isolation process was conducted for 15 min at 100 °C and was repeated three times for the same plant sample. Our previous work showed that microwave-ultrasonic agitation enhances the EO yield. Also, a short extraction period due to agitation is an advantageous point [22].

The obtained EO was collected into a clean beaker, chemically dried, and stored at 2–8 °C. The obtained EO yield average percentage was 0.95% from the dried plant sample.

2.2. GC–MS analysis

The EO of the (DV) plant was analyzed by GC–MS using a Perkin Elmer Clarus 500 GC gas chromatograph equipped with Perkin Elmer Clarus 560 mass spectrometer. The separation was performed by Perkin Elmer Elite-5 fused-silica capillary column (30 m x 0.25 mm, film thickness 0.25 μm). The column temperature was programmed and regulated from 50 °C for 5 min to 280 °C at 4 °C/min. The flow rate of helium as a carrier gas was set to 1 ml/min and was kept constant for all the chromatographic runs. 0.2 μl neat oil was injected in split mode with a split ratio of 1:50 and at a temperature of 250 °C. The components of the sample were classified by matching their mass spectra with those from the library; on the other hand, the pure standard components were confirmed by their GC retention times [22]. The RIs were experimentally calculated utilizing the standard method involving retention time (RT) of *n*-alkanes, which were injected under the same chromatographic conditions.

In brief, retention indices (RIs) have been calculated according to the injected standard mixture of normal alkanes (C6-C27) under the mentioned conditions using the following well-known equation approved by the International Union of Pure and Applied Chemistry (IUPAC) (https://goldbook.iupac.org/terms/view/R05360).

The identification was also confirmed by comparison of their mass spectra with those stored in the Wiley7n.l MS computer library. The linear temperature programmed RIs of all the constituents were calculated from the gas chromatogram by interpolation between bracketing n-alkanes using equation RI=100 × (((tRi-tRz)/(tR(z + 1)-tRz))+z); where z is the number of carbon atoms in the smaller n-alkane, tR(i), tR(z) and tR(z + 1) is the retention times of the desired compound, the smaller n-alkane and the larger n-alkane, respectively. Analysis of EO of the (DV) plant was deemed necessary since it might be interesting from an aromatherapy point of view.

2.3. DPPH radical scavenging activity

The donation ability of hydrogen atoms or electrons of the EO were estimated from the bleaching of a purple-colored methanol solution of DPPH. Nevertheless, the stock solution of the EO of the (DV) plant leaves and the Trolox were dissolved in methanol at 1 mg/ml concentrations. Each one of these stock solutions was diluted in methanol in the following concentrations: 2, 5, 10, 20, 50, 100 μg/ml. A new solution for the DPPH solution was dissolved in methanol at 0.002% w/v concentration. The working solutions of (DV) EO were mixed with methanol and DPPH at a fixed ratio of 1:1:1.

Meanwhile, a negative control solution was made by mixing the above mentioned DPPH solution with methanol only in a 1:1 ratio. All the solutions mentioned above were incubated for 30 min at 25 °C in a dark place. The UV–visible spectrophotometer at a wavelength of 517 nm was used to estimate the optical density of all studied samples. The antioxidant activity of (DV) EO and the reference compound (Trolox) were calculated by using the following formula:

The inhibition (%) of DPPH activity = (AB-AE)/AB × 100%,

Where: AB = Absorbance of the blank and AE = Absorbance of the EO.

The IC_{50} (antioxidant half-maximal inhibitory concentration) of (DV) EO and Trolox as well as their standard deviations, were calculated by using BioDataFit edition 1.02 [23].

2.4. Total phenolic content (TPC)

Soxhlet extractor was used in the extraction of phenolic compounds. Briefly, to (12 g.) of plant powder, 250 ml of 70% MeOH was added and refluxed for three hours. The solvent was then evaporated using a rotary evaporator and the residue (32% of dried extract) was kept in a refrigerator away from light. This was used for TPC and TFC determination, as well as for the neuroprotective tests.

TPC was determined by the Folin-Ciocalteu method [**24**], which is briefly as the following: A standard gallic acid calibration curve was constructed by preparing the dilutions (90–900 ppm). 1.800 mL of Folin-Ciocalteu reagent was added to 40 μL standard or sample (162.3 mg of extract 100 mL 20% EtOH). After 5 mins, 1.200 mL of 7.5% Na_2CO_3 solution was added. The solutions were incubated at 27 ˚C for 60 mins and then measured at 765 nm using Biochem Libra S22 UV–VIS spectrophotometer.

2.5. Total flavonoids content (TFC)

Aluminum chloride complex-forming assay was used to determine the TFC of the extracts [25]. Rutin was used as a standard for the calibration curve with concentrations (5–100 ppm). 300 μL of 5% $NaNO_2$ solution was added to 1500 μL standard or 100 μL sample (254.9 mg of extract in 100 mL 20% EtOH). After 5 mins, 300 μL of 10% $AlCl_3$ solution was added and the mixture was allowed to stand for 6 mins. Then 2000 μL of 1 M NaOH solution was added and 3000 μL of H_2O only to sample solutions. The absorbance of these mixtures was recorded at 510 nm using Biochem Libra S22 UV–VIS spectrophotometer.

2.6. FRAP assay

Antioxidant capacity was determined by FRAP (ferric reducing antioxidant power) method [25], which depends on the reduction of Fe^{+3} to Fe^{+2} by antioxidants producing blue-colored solution. Briefly, 1000 μL of FRAP solution and 1000 μL H_2O were added to 80 μL of standard or sample. The absorbance was recorded after 15 min at 593 nm spectrophotometrically.

2.7. HEK293 cell culture and transfection

All homomeric and heteromeric AMPARs subunits are in the flip isoform in pBlueScript and acquired from S. F. Heinemann (Salk Institute, La Jolla, CA). Both forms were subcloned in pRK for the expression in HEK293. The GluA2 unedited form (R607Q) (flip isoforms) and enhanced green fluorescent protein (EGFP) in pRK5 were a gift from P. H. Seeburg (Max Planck Institute for Medical Research, Heidelberg, Germany). Homomeric AMPAR plasmids were cotransfected with an EGFP expression vector at a ratio of 1 μg of GluA1–4 to 1 μg of GFP in HEK293 cells. Likewise, heterologous AMPAR plasmids were transfected in the same manner under a 1:2 ratio. Cells were then plated in Petri dishes of DMEM supplemented with 10% fetal calf serum and antibiotics and kept in a humidified incubator at 37 ˚C and 5% CO_2. Highly fluorescent cells were recognized and selected for recording. As for cell culturing and transfection, HEK293 (Sigma, Germany) were grown in a medium of DMEM, Dulbecco Modified Eagle Medium, (Sigma, USA) which contained 0.1 mg/ml streptomycin, and 1 mM sodium pyruvate (Biological Industries; Beit-Haemek, Israel) and a 10% of FBS, fetal bovine serum. The cells were sub-cultured about two times a week. The incubation time of HEK293 cells before transfection was 24 h set at 37 ˚C, 5% CO_2. The cells were left for 36 hrs in the incubator before the chemical transfection jetPRIME (Polyplus: New York, NY) was utilized. The cells were replated from the 12-well plates to coverslips coated with Laminin (1 mg/mL; Sigma, Germany) [26], preparing them for whole-cell patch-clamp recording. (See supplementary information for the methodology of DNA preparation).

2.8. HEK293 cell patch-clamp recordings

To perform the electrophysiology recording we used IPA (Integrated Patch Amplifier) (Sutter Instruments, Novato, CA) to calculate the inhibition, desensitization, and deactivation specific for the whole-cell patch-clamp technique. After two to three days of transfection, the HEK293 cells were recorded at a temperature of 22 ˚C with a membrane potential of −60 mV. To digitalize the membrane currents SutterPatch Software v. 1.1.1 (Sutter Instruments) was used whereby the sampling frequency was set at 10 kHz, while the low-pass filter was set to 2 kHz. Borosilicate glass was used to fabricate the Patch electrodes with a resistance of 2–4 MΩ. Additionally, data acquired were analyzed using Igor Pro7 (WaveMetrics, Inc.). The extracellular solution contained (values are in mM): 150 NaCl, 2.8 KCl, 0.5 $MgCl_2$, 2 $CaCl_2$, 10 HEPES adjusted to pH 7.4 with NaOH. while the solution that was continuously being supplied to the cells from a pipette contained (values are in mM): 110 CsF, 30 CsCl, 4 NaCl, 0.5 $CaCl_2$, 10 Trypsin EDTA solution B (0.25%), EDTA (0.05%), 10 HEPES, adjusted to pH 7.2 with CsOH.

Glutamate was first supplied to the cell to obtain the controlled current by using double-barrel glass (theta tube shape). Once recorded, one of the barrels was closed, and another one was opened to supply the cells with Inula viscosa and glutamate. Afterward, an identical protocol was done to produce the same glutamate-induced current to guarantee the safety of the cell. The theta tube was fixed on a high-speed piezo solution switcher (Automate Scientific, Berkeley, CA) to mirror the speed of naturally induced AMPAR currents. The 10%−90% solution exchange was typically less than 500 ms. Receptor desensitization (τdes) and deactivation rates (τdeact) were measured by applying glutamate for 500 ms and 1 ms, respectively. They were calculated by two exponential fittings of the current decay, starting from 95% of the peak to the baseline current. The weighted tau (τw) was calculated as $\tau w = (\tau f \times af) + (\tau s \times as)$, where (af) and (as) are the relative amplitudes of the fast (τf) and slow (τs) exponential component [27,28]. Every experiment was reproduced in cells obtained from at least 3–4 independent transfections, and the whole number of recorded whole-cell patches is shown in the corresponding figure legends.

3. Results

3.1. Phytochemical components

The EO of the (DV) plant was characterized by utilizing the GC–MS technique. Twenty-one phytochemical ingredients, representing 100% of the (DV) EO, were recognized and Patchulane, 3-b-Phenoxy-24-nor-cholan-5,20(22)-diene, 3-Ethyl-3-hydroxy-5alpha-androstan-17-one and γ-Gurjunene were the major components of the EO as shown in Table 1. (See supplementary information on GC–MS chromatogram in Figure S1).

3.2. Antioxidant activity

The DPPH assay was undertaken to estimate the free radical scavenging activity and the outcomes show that the (DV) EO has strong antioxidant potentials with an IC_{50} value of 13.5 ± 0.44 in comparison with Trolox which employed as a positive control that has an IC_{50} dose of 3.23±0.92 µg/ml as shown in Table 2 and Fig. 1.

3.3. Total phenolic content (TPC)

Measurements were performed in triplicate and results are given with standard deviation. Results showed high TPC (193.07 ± 9.1 mg Gallic acid eq./g extract), which is similar to those results obtained for Moroccan (140 - 274 GAE/g) [29] and Turkish plants (177 mg GAE/g) [30].

Table 1
Phytochemical constituents of (DV) EO and their classification percentage.

Common names	R.T	R.I $_{calc.}$	R.I. $_{Litr.}$	% of Area
β-Damascenone	25.74	710	710	0.01
Pent-1-yn-1-ylcyclohexane	26.42	700	699	0.03
L-camphor	26.42	705	705	0.03
Chloroacetic acid, dodec-9-ynyl ester	26.93	756	755	0.03
1,3,3-Trimethyl-2-hydroxymethyl-3,3-dimethyl-4-(3-methylbut-2-enyl)-cyclohexene	27.93	865	864	0.12
1-Formyl-2,2-dimethyl-3-trans-(3-methyl-but-2-enyl)–6-methylidene-cyclohexane	27.93	832	833	0.12
2-Methyl-3-(3-methyl-2-butenyl)–2-(4-methyl-3-pentenyl)oxetane	27.93	855	856	0.12
2-methyl-2-hydroxy-decalin-4A-carboxylic acid,2,4A-lactone	28.45	872	872	0.85
Naphthalene, 1,2,3,4,4a,5,6,7-octahydro-4a-methyl-2,2-diphenyl-	28.45	849	850	0.85
Spiro[4.5]decane-6-One	28.45	849	848	0.85
Tricyclo[4.4.1.0(1,6)]undecane	28.45	850	850	0.85
1-Methylene-2b-hydroxymethyl-3,3-dimethyl-4b-(3-methylbut-2-enyl)-cyclohexane	32.09	912	912	0.86
4-methoxy-6-methyl-6,7-dihydro-4H-furo(3,2-c) pyran	39.13	888	888	1.71
(28Z)–28-Heptatriaconten-2-one	39.13	841	840	1.71
Patchulane	40.36	739	739	22.82
3-b-Phenoxy-24-nor-cholan-5,20(22)-diene	40.36	734	733	22.82
3-Ethyl-3-hydroxy-5alpha-androstan-17-one	40.36	789	789	22.82
γ-Gurjunene	40.36	736	736	22.82
Hentriacontane	53.79	907	906	0.20
Sulfurous acid, butyl heptadecyl ester	53.79	815	814	0.20
Tritetracontane	53.79	827	827	0.20
Total				100
Category			Percentage	
Monoterpenoids			0.15%	
Sesquiterpenoides			46.74%	
Steroids			45.64%	
Others			7.49%	
Total			100%	

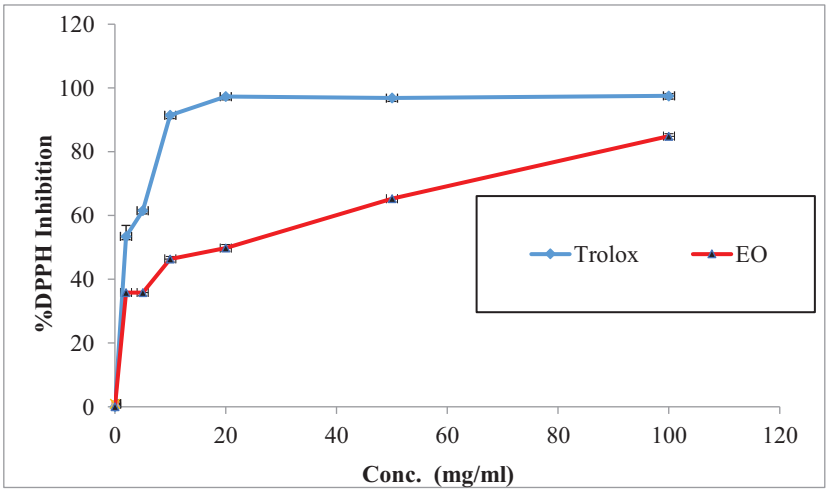

Fig. 1. DPPH inhibitory activity of the (DV) plant EO and Trolox.

Table 2
DPPH inhibitory activity and IC_{50} values of the (DV) plant EO and Trolox.

Conc.	Trolox	EO
0	0 ± 0.00	0 ± 0.00
2	53.43 ± 1.46	35.85 ± 0
5	61.51 ± 0.34	35.85 ± 0
10	91.41 ± 0.34	46.41 ± 0.75
20	97.29 ± 0.34	49.78 ± 1.11
50	96.8 ± 0.34	65.28 ± 0
100	97.54 ± 0.69	84.9 ± 0.75
Antioxidant activity IC_{50} (µg/ml), ±SD	3.23 ± 0.92	13.5 ± 0.44

Our results are a bit higher than those obtained in a study in Palestine (97.6–149.8 and 152.7–173.1 mg GAE/g for ethanolic and methanolic extracts, respectively) [31]. This difference may be attributed to the season of crop, extraction solvent and/or location of the plant. (See supplimentary information in Figure S2 for the calibration curve of gallic acid for the calculation of TPC).

3.4. Total flavonoids content (TFC)

High TFC value was detected in our samples (594.9 ± 12.2 mg RE/ g extract). Other studies showed high content, but expressed in quercetin equivalent (QE/g extract) [30,31,32], while our results are expressed as rutin equivalent. (For more information, see supplimentary Figure S3 for rutin standard curve from which TFC was calculated).

Additionally, high antioxidant values were obtained from the FRAP test (139.8 ± 2.3 mg Fe/g dry extract). Figure S4 shows the standard curve for ferrous absorption.

3.5. Effect of the (DV) plant EO on the amplitude of AMPAR subunits

The Heterologous (GluA1/2, GluA2/3) and Homologous forms of AMPARs subunits were all analyzed via HEK293 cells, to observe the

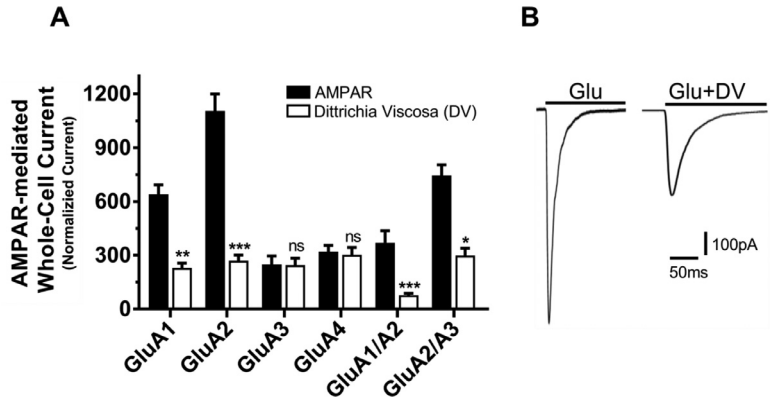

Fig. 2. Effect of *Dittrichia Viscosa* on the peak current of AMPAR subunits.

effect of (DV) plant EO on the amplitude generated by different AMPARs. Previously, a 10 mM ligand concentration was determined by a ~95% equivalence to an open-channel state of the receptor [26]. Also, the effect of (DV) on the Sub-AMPA receptors was determined at a fixed concentration of 231.4 (mg/10.0 ml), which was chosen so to obtain the highest efficacy without damaging the health of the cells. The amplitude and biophysical gating properties generated by the AMPARs were determined using Integrated Patch Amplifiers (IPA) to provide efficient low-noise whole-cell recordings. Meanwhile, the (DV) was applied on AMPAR by utilizing piezo fast exchange solution. Data were analyzed using Igor 7 software.

The peak current was reduced in some of the AMPARs and not others suggesting selective inhibition to specific AMPAR subunits upon the administration of (DV). The amplitude of AMPA receptors subunits without (DV) treatment; 640 ± 53 pA, 1105 ± 94 pA, 250 ± 46 pA, 320 ± 35 pA, 370 ± 67 pA, and 745 ± 59 pA for GluA1, GluA2, GluA3, GluA4, GluA1/2, and GluA2/3, respectively as shown in Fig. 2A. However, with the (DV) treatment, the current peak was reduced for GluA1, GluA2, GluA1/2, and GluA2/A3 to the following recordings; 229 ± 27 pA, 270 ± 31 pA, 77 ± 11 pA and 298 ± 42 pA. As for GluA3 and GluA4 (DV) had no notable changes in the amplitude produced by these AMPAR subunits, which recorded at 245 ± 39 pA, 302 ± 41 pA. Fig. 2B highlights the current traces generated by GluA2 with and without the administration of (DV) due to having the highest significant inhibition in comparison to other AMPARs.

Stabilizing the environmental conditions (−60 mV, pH 7.4, and 22 ˚C) to conduct the whole-cell current of homologous and heterologous AMPAR expressing HEK293 cells. The activation of the receptor is represented in the graph, i.e. weighted time constants. The current was calculated by averaging the mean of 5 samples (1 cell/trail). One-way ANOVA test was used with a significant of * $p < 0.05$; ** $p < 0.01$; and *** $p < 0.001$, while the not significant result was abbreviated as (ns). **A.** Amplitude generated by different AMPARs subunits without the administration of (DV) (left) vs. (DV) treatment (right). The time per recording is set at 500 ms after the application of 10 mM of the ligand. **B.** A comparative analysis for the traces of whole-cell currents from the most effected AMPAR subunit. The first trace represents homologous GluA2 alone without the effect of (DV), while the significant drop in current in the second trace is a representative of (DV) induced by the GluA2 subunit.

3.6. (DV) EO alters AMPAR desensitization in a subunit-dependent manner

Investigating the inhibition of (DV) on AMPAR activity prompted the curiosity of its influence on the receptor's desensitization rate (Fig. 3). Prior to any treatment the meantime of desensitization for GluA1, GluA2, GluA3, GluA4, GluA1/2 and GluA2/3 were as follows: 2.9 ± 0.1, 2.4 ± 0.1, 3.3 ± 0.4, 2.9 ± 0.3, 5.7 ± 0.4, and 2.6 ± 0.2 (ms) signifying the rate (τ=1/ms) of 0.34, 0.42, 0.30, 0.34, 0.17, 0.38 (ms-1), respectively (Fig. 3A-left). Nonetheless, the declined desensitization rate was expressive in GluA1 and GluA2 homologous AMPARs only, while for heterologous AMPARs both forms were significant upon treating the cells with (DV). Hence, desensitization increased to 3.6 ± 0.3, 4.4 ± 0.4, 6.7 ± 0.6, and 3.4 ± 0.4 (ms) which, as a result, reduces the desensitization rates to 0.28, 0.23, 0.15, and 0.29 (ms-1), respectively (Fig. 3A-right). On the contrary, no observable effect was seen for the desensitization of GluA3 and GluA4 upon applying (DV) to the cells expressing these AMPAR subunits. Hence, the readings were 3.5 ± 0.4 ms for GluA3 and 3.0 ± 0.5 ns ms for GluA4. Fig. 3B showcases the current traces generated by GluA2 with and without the administration of the EO due to having the most significant reduction in the desensitization rate in comparison to other AMPARs.

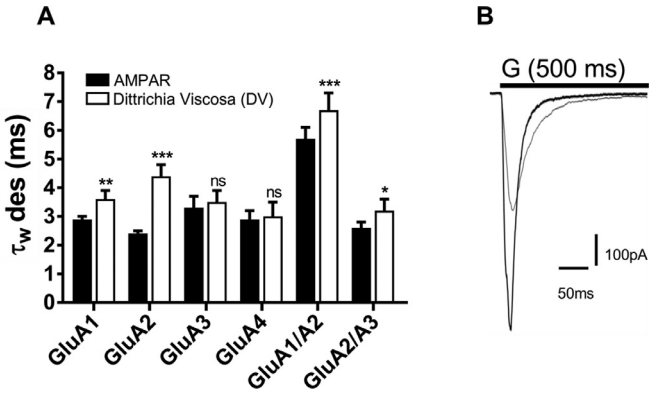

Fig. 3. Effect of EO on AMPAR desensitization.

Stabilizing the environmental conditions (−60 mV, pH 7.4, and 22 ˚C) to conduct the whole-cell patch-clamp of homologous and heterologous AMPAR subunits expressing in HEK293 cells. The desensitization of the receptor is represented in the graph, i.e. the current decay was calculated by a single exponential fitting a 95% of the peak to the baseline current. One-way ANOVA test was used with a significant of * $p < 0.05$; ** $p < 0.01$; and *** $p < 0.001$, while the insignificant result was abbreviated as (ns). **A.** The desensitization rate generated by different AMPARs subunits without the administration of (DV) (left) vs. (DV) treatment (right). The time per recording was set at 500 ms after the application of 10 mM of the ligand. **B.** Current traces of the most affected AMPAR subunit, i.e., GluA2, in HEK293 cells.

3.7. (DV) EO changes AMPAR deactivation rate

The results of (DV) on AMPAR's desensitization kinetics prompted the investigation of the EO impact on AMPAR deactivation (Fig. 4). The effect on deactivation from (DV) was similar to the effect observed on desensitization, in that it was selective to certain subunits. Thus, the

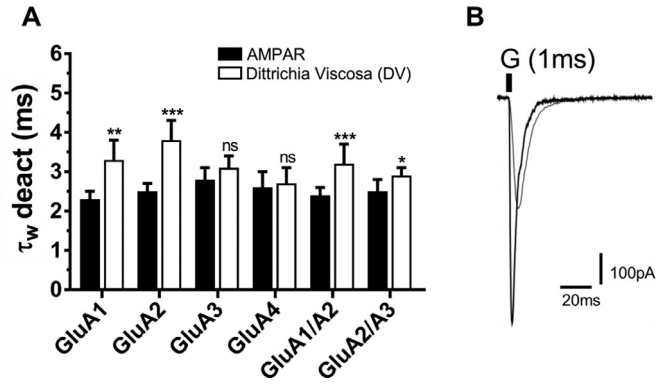

Fig. 4. Results from the effect of *Dittrichia Viscosa* on AMPAR deactivation.

average deactivation time for GluA1, GluA2, GluA3, GluA4, GluA1/2 and GluA2/3 recorded at; 2.3 ± 0.2 ms, 2.5 ± 0.2 ms, 2.8 ± 0.3 ms, 2.6 ± 0.4 ms, 2.4 ± 0.2 ms, and 2.5 ± 0.3 ms, denoting an average rate (τ = 1/ms) of 0.43 ms-1, 0.40 ms-1, 0.36 ms-1,0.38 ms-1, 0.42 ms-1, and 0.40 ms-1, respectively. Much like the desensitization, the average deactivation rate for GluA3 and Glu-A4 did not significantly change with the application of EO to the cells expressing such subunits. Hence, the deactivation was recorded at 3.1 ± 0.3 ms for GluA3 at a rate of 0.32 ms-1; similarly, GluA4 deactivation was recorded at 2.7 ± 0.4 ms at a rate of 0.37 ms-1. However, the deactivation rate was significantly reduced for GluA2 and GluA1/2, recording at 3.8 ± 0.5 ms and 3.2 ± 0.5 ms denoting the average deactivation rate as 0.26 ms-1 and 0.32 ms-1, respectively. Likewise, the deactivation of GluA1 increased to 3.3 ± 0.5 ms, resulting in a decrease in the average rate of desensitization to 0.30 ms-1. Finally, GluA2/3 had a small change in deactivation upon (DV) administration to equal 2.9 ± 0.2 ms, denoting a decreased average rate of 0.34 ms-1.

Maintaining the environmental conditions (−60 mV, pH 7.4, and 22 ˚C) to conduct the whole-cell current of homologous and heterologous AMPAR subunits expressing in HEK293 cells. The deactivation of the receptor is represented in the graph, i.e. deactivation was fitted with two exponentials as $\tau w = (\tau f \text{ x af}) + (\tau s \text{ x as})$. The deactivation rate was calculated by averaging the mean of 5 samples (1 cell/trail). One-way ANOVA test was used with a significant of $^{*}\ p < 0.05$; $^{**}\ p < 0.01$; and $^{***}\ p < 0.001$, while not significant result was abbreviated as (ns). **A.** deactivation rate generated by different AMPARs subunits without the administration of (DV) (left) vs. (DV) treatment (right). The time per recording is set at 500 ms after the application of 1 mM of the ligand. **B.** Current traces of the GluA2, i.e., most affected AMPAR subunit. (See Table S1 for data analysis for the whole-cell recordings).

4. Discussion

4.1. Phytochemical components and antioxidant activity

The GC–MS characterization revealed that the EO contains several classes of phytochemical compounds including essential oils that compromise 45.686% of the total identified compounds. However, the major compounds of these essential oils are patchulane and γ-gurjunene representing 22.826% for each compound. In addition, 54.314% are non-volatile oils that are mainly composed of 3-b-Phenoxy-24-nor-cholan-5,20 (22)-diene (22.826%) and 3-Ethyl-3-hydroxy-5alpha-androstan-17-one (22.826%). In addition, the results of the antioxidant screening provide a strong motive for further investigating DV as a neuroprotective agent. Consequently, antioxidant compounds are those that inhibit oxidation; free radicals can be produced by this chemical reaction, which may cause damage to cells of organisms [29]. Therefore, antioxidant products can prevent a broad range of diseases including Alzheimer's, cancer, cardiovascular and macular degeneration. Further studies indicate the importance of antioxidants in preventing and slowing the progression of several neurodegenerative diseases including ALS PD and AD. In this study, we show that the EO of the (DV) plant has high potential antioxidant activity when compared to the positive control, Trolox. A recent study conducted by Chahmi et al. found that the ethanol and ethyl acetate extraction of the (DV) plant collected from Morocco has also a potent antioxidant activity with 0.27 and 1.86 g/l, respectively [29]. Table 3 shows a literature review of methods of extraction, and analysis as well as for main components of (DV) EO.

4.2. Neuroprotective effect

AMPARs are accountable for the majority of excitatory neurotransmission in the CNS and have a critical role in brain function such as memory and learning formation as well as induction and maintenance of long-term potentiation (LTP) and long-term depression (LTD) that is involved in synaptic plasticity [11]. The activation of AMPARs only requires glutamate, opening the channel on a microsecond domain time scale; however, they undergo profound desensitization on the millisecond timescale [33]. Desensitization is caused by ion channel pore closure, while the ligand is still bound to the receptor. On the other hand, deactivation of AMPARs is described as the natural decay in current after the release of ligand (glutamate) from the receptor and closure of the channel gate [12,34]. Excessive AMPAR activation has been linked to glutamate toxicity, which is associated with the pathogenesis and progression of various neurodegenerative diseases [9,18]. Various research has investigated possible AMPAR antagonists to reduce neuronal loss, however, to this date there is only one successful inhibitor of the receptor acting as an anticonvulsant [16]. Nonetheless, researchers persevere to synthesize a drug with greater neuroprotective properties and reduced side effects by targeting AMPARs.

The pharmaceutical drug currently in the market known as perampanel is used as an antiepileptic drug but has severe numerous side effects such as depression, anxiety, paranoia, weight gain, joint and back pain [17,19]. In response, this research studies a popular Mediterranean plant, (*DV*), used in traditional medicine and researched in various medical fields such as cancer [1,2]. Little is known regarding its effect on neurodegenerative diseases, specifically concerning neurotoxicity. After performing whole-cell patch-clamp electrophysiology to record the peak current, desensitization and deactivation of various AMPAR subunits with and without the presence of the EO on HEK293 cells, we observed a selective inhibition, reduced desensitization and deactivation rates of specific AMPAR subunits. For GluA2 and GluA1 homomer and GluA1/2 and GluA2/A3 heteromeric AMPARs, (DV) inhibited their activity by 2.8, 4.1, 4.8 and 2.5 folds, respectively. They also reduced both deactivation and desensitization rates, notably, indicating the property to slow the kinetics of those receptors and further improve its neuroprotective properties. Hence, a common mechanism is observed between these receptors in response to (DV) that affect all biophysical gating properties. However, the homotetramers of GluA3 and GluA4 AMPAR subunits were not affected by (DV) on any of the tested biophysical properties (peak current, desensitization or deactivation) meaning the action of (DV) is subunit dependent. Moreover, the action of (DV) is of synergetic effect, which translates to doubling the inhibition of GluA1 and GluA2 once they are in the heterogenic form while reducing the inhibition of GluA2 by half once it is combined with GluA3 heterogenic form as (DV) deployed no effect on that subunit. These results imply that the mechanism of inhibition observed by (DV) is through the binding on an allosteric site-specific only to GluA1 and GluA2 AMPA subunits. Thus, the site of interaction on AMPARs for (DV) is amino acid sequence-specific, and the interaction between (DV) and GluA2 is of more excellent stability than GluA1 as it provided a higher level of inhibition.

Recent X-ray crystal structures of AMPARs indicated the binding sites of its antagonists to be in the linker regions, namely S1-M1 and S2-M4, which cause the stabilization of the closed channel state [35,36]. Hence, the results of the current study suggest that the interaction between the receptor and (DV) is related in amino sequence whereby GluA3 and

Table 3
Literature review of (DV) EO from different regions.

Region	Method of extraction	Method of analysis	Main components	References
Algeria	Steam distillation	GCMS using a Hewlett Packard 6890 GC coupled to a Hewlett Packard 5973 mass spectrometer	Isocostic acid (56.83%), fokienol (14.6%), and butyl hydroxy-toluene (2.26%)	Madani, L., Derriche, R., Haoui, I.E. (2014). Essential oil of Algerian Inula viscosa leaves. J. Essent. Oil Bearing Plants. 17(1): 164–168.
Algeria	Hydrodistillation	GC–MS analyses of the oil samples were carried out on a Hewlett–Packard 6890 N gas chromatograph coupled to an HP 5973 mass selective detector (MSD)	12-carboxyeudesma-3,11 (13) diene (28.88%); linolenic acid (7.80%); palmitic acid (5.38%); butyl hydroxy toluene (4.11%) and fokienol (3.37%)	Haoui, I.E., Derriche, R., Madani, L., Oukali, Z. (2015). Analysis of the chemical composition of essential oil from Algerian Inula viscosa (L.) Aiton. Arabian J. Chem. 8(4): 587–590
	Steam distillation		12-carboxyeudesma-3,11 (13) diene (56.81%); 2,3-didehydrocostic acid (3.25%); butyl hydroxy toluene (2.63%) and pentacosane (2.31%)	
Turkey	Hydrodistillation	GC was carried out on a Varian 3300 gas chromatograph fitted with a fused silica	Borneol (25.2%), bornyl acetate (19.5%) and isobornyl acetate (22.5%)	Perez-Alonso, M.J., Velasco-Negueruela, A. (1996). Composition of the volatile oil from the aerial parts of Inula viscosa (L) Aiton. flavor Fragr. J. 11: 349–351.
Italy	Hydrodistillation	Capillary GCMS, Hewlett Packard 6890–5973 MSD controlled by chemstation software and equipped with an HP 6890 Series Injector autosampler	12-carboxyeudesma3,11(13)-diene (44%), selina α–6-en-4-ol (7%), caryophyllene oxide (3%), and α–eudesmol (3%)	De laurentis, N., Losacco, V., Milillo, M.A. (2002). Chemical investigations of volatile constituents of Inula viscosa (L) Aiton (Asteraceae) from different areas of Apulia, Southern Italy. Delpinoa n.s. 44: 115–119.
Jordan	Hydrodistillation	Hewlett Packard HP-8590 gas chromatograph equipped with a split-splitless injector (split ratio, 1:50) and an FID detector	Fokienol (20.87%), (E)-nerolidol (19.75%), β–Eudesm-6-en-4α-ol (5.64%), α-Vetivone (3.60%), α-Eudesmol (2.68%) and Caryophyllene oxide (2.57%)	Al-Qudah, Mahmoud A., Hala I. Al-Jaber, and Abdulraouf S. Mayyas. "Chemical compositions of the essential oil from the Jordanian medicinal plant Dittrichia viscosa." Jordan Journal of Chemistry 146.600 (2010): 1–6.
Portugal	Hydrodistillation	GC and GC–MS using fused silica capillary columns with two stationary phases	Fokienol (11.8%), T-muurorol (7.9%), (E)-nerolidol (5.5%) and δ-cadinene (5.0%)	Antimicrobial Activity of the Essential Oils of Dittrichia viscosa subsp. viscosa on Helicobacter pylori

GluA4 have a reduced affinity to (DV) in comparison to GluA1 and GluA2. X-ray crystal structures demonstrated the antagonist sites of AMPARs to be in the M regions of the linkers. More importantly, point mutation studies have demonstrated 9 residues to be specifically involved in interacting with various antagonists. The amino residues are dispersed throughout the linker regions of the receptor, 4 of which are located at the PreM1region; F517, P520 (nonpolar) S516 (Polar) and D519 (negatively charged), while 3 other amino residues located at the M3 region; L620 & F623 (nonpolar), Y616 (Polar), finally the last residues located at the M4 region are; S788 and N791 (Polar) [37].

In comparison to other studies published by our laboratory that focus on the effect of essential oils on the biophysical gating properties of AMPARs, (DV) showed significant levels of inhibition against AMPARs. Unlike *Lavandula dentata* L. and *Origanum syriacum* L. essential oils [27], both of which alerted the desensitization and deactivation rate of all AMPAR subunits but not the current peak. The current study provides depressing activity on specific AMPAR subunits, namely, GluA1 and GluA2. Interestingly, the action of the impact seen of (DV) as a possible antagonist for AM38PARS is similar to the curcumin derivatives synthesized by our labs [28,38], in that they affected all gating properties. However, while the curcumin derivatives were sub-unit independent like perampanel, the results of (DV) is like the drug talampanel that targets specific AMPARs subunits. However, talampanel failed in a clinical phase II trial as a possible ALS drug due to its ineffectiveness on GluA3 AMPARs both in the heteromeric and homomeric form [37]. Contrary, due to the synergetic effect observed by (DV) which talampanel lacked, its effect on GluA3 subunits is efficient if it were in a heterogenic form.

Competitive inhibitors compete with glutamate for the ligand-binding site, to impact activation; noncompetitive inhibitors have allosteric sites that modulate the activity independent of glutamate concentration. The effect of (DV) seems to non-competitively inhibit AMPARs as an increase in glutamate concentration had no visible effect on the level of inhibition observed by the treatment of (DV). The inhibition of AMPARs may be attributed mainly to the flavonoids present in *Inula* extract [39]. The structure reveals the polyphenolic moieties that are able to establish a hydrogen bonding with either the S1-M1 and/or S2-M4 linkers. This non-competitive binding stabilizes their closed conformation, preventing gating of the channel when an antagonist is bound to the ligand-binding domain [38].

AMPA receptors have an essential role in the pathophysiology of many neurological disorders, as mentioned above. Reducing the activity of these receptors has remedial effects on neurologic diseases and (DV) shows such characteristics that could be encouraging for future drug synthesis. Moreover, the results of the current study provide insight to better understand the function of different AMPAR subunits, their unique makeup, and the consequences of such phenomena. The limitation of this study is the inability to locate the specific region of interaction between the antagonist and AMPARs. Nonetheless, in support of recent studies that highlight the impact of specific AMPAR subunits on different neuropsychological diseases the results of the study promise a target for diseases linked specifically to GluA1 and GluA2 over-expression and activity. For example, (DV) intensely affected GluA2 containing AMPARs the most, which is of critical importance to neurodegenerative diseases specific to GluA2 receptors such as ALS and Fragile X Syndrome [21,35]. Finally, when comparing the effect of DV on homomeric vs. heteromeric AMPAR subunits, a significant difference is observed which further support the mechanism of action of (DV) to be subunit dependent, hence, the allosteric site of (DV) is specific in amino sequence, implementing the effect in a synergetic fashion [38,40].

5. Conclusion

The GC–MS characterization of the (DV) plant EO showed the presence of various classes of phytochemical molecules, including essential oils. In addition, this EO revealed strong antioxidant activity compared to Trolox. Antioxidant activity is attributed to the high content of both phenolics and flavonoids present in the extract, showing high TPC and TFC values. Moreover, the study reveals the inhibitory properties of (DV) EO and a higher neuroprotectivity property via an increase in the desensitization and deactivation of specific AMPA receptors. The gating properties of the most effected AMPAR subunits were GluA2, followed by GluA1/A2, GluA1, and GluA2/3, respectively, suggesting the inhibition was subunit dependent. On the other hand, the homotetramer of GluA3 and GluA4 were not affected by (DV), suggesting the interaction between antagonist and AMPAR is specific to the subunit amino sequence. Moreover, glutamate concentration appeared to have no remarkable effect on inhibition, suggesting the mechanism of (DV) acts as a non-competitive antagonist. Besides, the desensitization and deactivation rates decreased in the same manner as the reduction in peak current, insinuating the action of (DV) targets all biophysical properties of the specific AMPAR subunits. Although the exact mechanism describing the effect of DV on AMPARs is absent from this study, we assume it is through the AMPAR to (DV) interaction via the linker regions of specific AMPAR subunits. Nonetheless, it is important to note other possible mechanisms such as reducing the post-synaptic AMPAR density by effecting AMPAR trafficking or influencing the ion permeability by altering the chemical structure of AMPAR ion channels. Thus, further research is needed to identify the specific interaction and effect of (DV) on AMPAR, yet, we confirm favorable inhibitory and neuroprotective properties of the EO on AMPARs as a potential candidate for excitotoxicity.

Authors contribution

Mohammad Qneibi, Michel Hanania: Conceptualization, Data curation, Formal analysis, Funding acquisition, Investigation, Methodology, Project administration, Resources, Software, Supervision, Validation, Visualization, Writing - original draft, Writing - review & editing.. **Nidal Jaradat:** Investigation, Methodology, Validation, Visualization, Writing - review & editing. **Nour Emwas, Sireen Radwan:** Investigation and Validation.

Financial support

Current work was financially support by a grant from The Palestinian Ministry of Education and Higher Education through Palestinian-German cooperation and An-Najah National University (Grant number: PALGER2017–009) and the Deanship of Research at Bethlehem University.

Declaration of Competing Interest

The authors declare that they have no conflict of interests. Nidal Jaradat is an Associate Editor of this journal.

Acknowledgments

The authors would like to acknowledge The Palestinian Ministry of Education and Higher Education through Palestinian-German cooperation and An-Najah National University for their support. The authors are also grateful to Dr. Omar Dar Issa to identify and verify the plant. Dr. Omar is a botanist (Associate Professor, Department of Biology, Bethlehem University, Bethlehem, Palestine).

Data availability

This is accessible to other authors upon request

Supplementary materials

Supplementary material associated with this article can be found, in the online version, at doi:10.1016/j.eujim.2021.101291.

References

[1] R. Bar-Shalom, M. Bergman, S. Grossman, N. Azzam, L. Sharvit, F. Fares, *Inula Viscosa* extract inhibits growth of colorectal cancer cells in vitro and in vivo through induction of apoptosis, Front. Oncol. 9 (2019) 227, doi:10.3389/fonc.2019.00227.
[2] H. Mohti, M.F. Taviano, F. Cacciola, P. Dugo, L. Mondello, A. Marino, G. Crisafi, Q. Benameur, A. Zaid, N. Miceli, *Inula Viscosa* (L.) aiton leaves and flower buds: effect of extraction solvent/technique on their antioxidant ability, antimicrobial properties and phenolic profile, Nat. Prod. Res. 34 (1) (2019) 46–52, doi:10.1080/14786419.2019.1569659.
[3] N.A. Orhan, D. Gökbulut, D. Orhan, Antioxidant potential and carbohydrate digestive enzyme inhibitory effects of five inula species and their major compounds, S. Afr. J. Bot. 111 (2017) 86–92, doi:10.1016/j.sajb.2017.03.040.
[4] I. Trimech, E.K. Weiss, V.S. Chedea, D. Marin, A. Detsi, E. Ioannou, V. Roussis, P. Kefalas, Evaluation of anti-oxidant and acetylcholinesterase activity and identification of polyphenolics of the invasive Weed Inula Viscosa, Phytochem. Anal. 25 (50) (2014) 421–428, doi:10.1002/pca.2510.
[5] W.R. Tavares, A.M.L. Seca, L Inula, Secondary metabolites against oxidative stress-related human diseases, Antioxidants 8 (5) (2019) 122, doi:10.3390/antiox8050122.
[6] N. Brahmi-Chendouh, S. Piccolella, G. Crescente, F. Pacifico, L. Boulekbache, S. Hamri-Zeghichi, S. Akkal, K. Madani, S. Pacifico, UHPLC-HR-MS/MS based polyphenol profile, and antioxidant and cytotoxic activities, J. Food Drug Anal. 27 (2019) 692–702, doi:10.1016/j.jfda.2018.11.006.
[7] S. Abuhamdah, R. Abuhamdah, S. Al-Olimat, P. Chazot, Phytochemical investigations and antibacterial activity of selected medicinal plants from Jordan, Eur. J. Med. Plants. 3 (3) (2013) 394–404, doi:10.9734/EJMP/2013/3540.
[8] L. Karygianni, M. Cecere, A.L. Skaltsounis, A. Argyropoulou, E. Hellwig, N. Aligiannis, A. Wittmer, A. Al-Ahmad, High-level antimicrobial efficacy of representative mediterranean natural plant extracts against oral microorganisms, Biomed. Res. Int. (2014) 839019, doi:10.1155/2014/839019.
[9] M.F. Beal, Mechanisms of excitotoxicity in neurologic diseases, FASEB J. 6 (15) (1992) 3338–3344, doi:10.1096/fasebj.6.15.1464368.
[10] A. Schousboe, Glutamate neurotoxicity related to energy failure, in: R.M. Kostrzewa (Ed.), Handbook of Neurotoxicity, Springer, New York, 2014, pp. 1299–1310.
[11] A. Wright, V. Bryce, The essential role of AMPA receptor GluR2 subunit RNA editing in the normal and diseased brain, Front. Mol. Neurosci. 5 (34) (2012) 1–13, doi:10.3389/fnmol.2012.00034.
[12] X. Dong, Y. Wang, Z. Qin, Molecular mechanisms of excitotoxicity and their relevance to pathogenesis of neurodegenerative diseases, Acta Pharmacol. Sin. 30 (4) (2009) 379–387, doi:10.1038/aps.2009.24.
[13] P.R. Heath, P.J. Shaw, Update on the glutamatergic neurotransmitter system and the role of excitotoxicity in amyotrophic lateral sclerosis, Muscle Nerve 26 (4) (2002) 438–458, doi:10.1002/mus.10186.
[14] A. Lau, M. Tymianski, Glutamate Receptors, Neurotoxicity and Neurodegeneration, Pflugers Arch -Eur. J. Physiol. 460 (2) (2010) 525–542, doi:10.1007/s00424-010-0809-1.
[15] K. Lee, L. Goodman, C. Fourie, S. Schenk, B. Leitch, J.M. Montgomery, AMPA receptors as therapeutic targets for neurological disorders, in: R. Donev (Ed.), Advances in Protein Chemistry and Structural Biology, Academic Press, New York, 2016, pp. 203–261.
[16] M. Espahbodinia, R. Ettari, W. Wen, A. Wu, Y. Shen, L. Niu, S. Grasso, M. Zappalà, Development of Novel N-3-Bromoisoxazolin-5-yl Substituted 2,3-Benzodiazepines as Noncompetitive AMPAR Antagonists, Bioorg. Med. Chem. 25 (14) (2017) 3631–3637, doi:10.1016/j.bmc.2017.05.036.
[17] C.L. Yuan, E. Shi, J. Srinivasan, C.P. Ptak, R.E. Oswald, L.M. Nowak, Modulation of AMPA receptor gating by the anticonvulsant drug, Perampanel. ACS Med. Chem. Lett. 10 (3) (2018) 237–242, doi:10.1021/acsmedchemlett.8b00322.
[18] W. Dai, X. Gao, D. Xiao, Y. Li, X. Zhou, Z. Yong, R. Su, The Impact and Mechanism of a novel allosteric AMPA receptor modulator LCX001 on protection against respiratory depression in rodents, Front. Pharmacol. 10 (2019) 10–14, doi:10.3389/fphar.2019.00105.
[19] H. Chiang, S. Lim, H. Hsieh, M. Cheng, C. Chang, W.J. Tseng, H.T. Li, C.Y. Lin, T. Wua, Preliminary Asian experience of using perampanel in clinical practice, Biomed. J. 40 (6) (2017) 347–354, doi:10.1016/j.bj.2017.09.003.
[20] J.E. Harms, M. Benveniste, M. Kessler, L.M. Stone, A.C. Arai, K.M. Partin, A charge-inverting mutation in the "linker" region of α-amino-3-hydroxy-5-methyl-4-isoxazolepropionic acid (AMPA) receptors alters agonist binding and gating kinetics independently of allosteric modulators, J. Biol. Chem. 289 (15) (2014) 10702–10714, doi:10.1074/jbc.m113.526921.
[21] C. Danesi, K. Keinänen, M.L. Castrén, Dysregulated Ca2+-Permeable AMPA receptor signaling in neural progenitors modeling fragile X syndrome, Front. Synaptic. Neurosci 1 (2) (2019) 1–8, doi:10.3389/fnsyn.2019.00002.
[22] N. Jaradat, S. Al-Lahham, M.N. Abualhasan, A. Bakri, H. Zaide, J. Hammad, F. Hussein, L. Issa, A. Mousa, R. Speih, Chemical constituents, antioxidant, cyclo-oxygenase inhibitor, and cytotoxic activities of teucrium pruinosum boiss. essential oil, Biomed. Res. Int. (2018) 1–9, doi:10.1155/2018/4034689.
[23] N. Jaradat, B. Damiri, M. Abualhasan, Antioxidant evaluation for Urtica urens, Rumex cyprius and Borago officinalis edible wild plants in Palestine, Pak. J. Pharm. Sci. 29 (2016) 325–330 https://www.researchgate.net/publication/303483780.

[24] M. Hanania, S. Radwan, E. Karmi, Extraction method and evaluation of phenolics, flavonoids, antioxidant activity, antimicrobial activity and minerals of bitter lupinus albus in Palestine, J. Biol. Act. Prod. Nat. 8 (2) (2018) 137–143, doi:10.1080/22311866.2018.1465355.

[25] S. Radwan, G. Handal, F. Rimawi, M. Hanania, Seasonal variations in antioxidant activity, total flavonoids content, total phenolic content, antimicrobial activity and some bioactive components of ficus carica L. in Palestine, Int. J. Pharmtech. Res. 13 (4) (2020) 329–340, doi:10.20902/IJPTR.2019.120404.

[26] M. Qneibi, N. Micale, S. Grasso, L. Niu, Mechanism of Inhibition of GluA2 AMPA Receptor Channel Opening by 2,3-Benzodiazepine Derivatives: functional Consequences of Replacing a 7,8-Methylenedioxy with a 7,8-Ethylenedioxy Moiety, Biochemistry 51 (8) (2012) 1787–1795, doi:10.1021/bi2017552.

[27] M. Qneibi, N. Jaradat, M. Hawash, A. Zaid, A. Natsheh, R. Yousef, Q. AbuHasan, The neuroprotective role of origanum syriacum L. and Lavandula dentata L. essential oils through their effects on AMPA receptors, Biomed. Res. Int. 2019 (2019) 1–11, doi:10.1155/2019/5640173.

[28] M. Qneibi, O. Hamed, O. Fares, N. Jaradat, A. Natsheh, Q. AbuHasan, N. Emwas, R. Al-Kerm, R. Al-Kerm, The inhibitory role of curcumin derivatives on ampa receptor subunits and their effect on the gating biophysical properties, Eur. J. Pharm. Sci. 136 (2019) 104951, doi:10.1016/j.ejps.2019.06.005.

[29] N. Chahmi, J. Anissi, S. Jennan, A. Farah, K. Sendide, M.El Hassouni, Antioxidant activities and total phenol content of inula viscosa extracts selected from three regions of Morocco, Asian Pac. J. Trop. Biomed. 5 (3) (2015) 228–233, doi:10.1016/S2221-1691(15)30010-1.

[30] A. Gökbuluta, O. Özhana, B. Satılmışb, K. Batçıoğlub, S. Günalc, E. Şarera, Antioxidant and antimicrobial activities, and phenolic compounds of selected inula species from Turkey, Nat. Prod. Commun. 8 (4) (2013) 475–478.

[31] H. Salim, W. Rimawi, A. Mjahed, Analysis of extracts from palestinian inula viscosa for their phenolic, flavonoid and lipid contents, antioxidant, antibacterial activity, J. Chem. Biochem. 5 (1) (2017) 12–23, doi:10.15640/jcb.v5n1a2.

[32] E. El Ouariachi, A. Bouyanzer, Antioxidant activity of solvent extracts of Inula viscosa from Morocco, Arab. J. Chem. Environ. Res. 1 (1) (2014) 33–40.

[33] M. Yennawar, R.S. White, F.E. Jensen, AMPA receptor dysregulation and therapeutic interventions in a Mouse model of CDKL5 deficiency disorder, J. Neurosci. 39 (24) (2019) 4814–4828, doi:10.1523/JNEUROSCI.2041-18.2019.

[34] N. Armstrong, J. Jasti, M. Beich-Frandsen, E. Gouaux, Measurement of conformational changes accompanying desensitization in an ionotropic glutamate receptor: structure of G725C Mutant, Cell 127 (1) (2006) 85–97, doi:10.1016/j.cell.2006.08.037.

[35] A. Hoffmann, E. Berry-Kravis, Autism spectrum disorders and intellectual disability: genetic and non-genetic causes, in: C. Sala, C. Verpelli (Eds.), Neuronal and Synaptic Dysfunction in Autism Spectrum Disorder and Intellectual Disability, Academic Press, New York, 2016, pp. 325–346.

[36] M. Qneibi, O. Hamed, A. Natsheh, O. Fares, N. Jaradat, N. Emwas, Q. AbuHasan, R. Al-Kerm, R. Al-Kerm, Inhibition and assessment of the biophysical gating properties of GluA2 and GluA2/A3 AMPA receptors using curcumin derivatives, PLoS ONE 14 (8) (2019) 1–15, doi:10.1371/journal.pone.0221132.

[37] C. Wang, L. Niu, Mechanism of inhibition of the GluA2 AMPA receptor channel opening by talampanel and its enantiomer: the stereochemistry of the 4-methyl group on the diazepine ring of 2,3-benzodiazepine derivatives, ACS Chem. Neurosci. 4 (4) (2013) 635–644, doi:10.1021/cn3002398.

[38] M. Qneibi, N. Jaradat, N. Emwas, Effect of geraniol and citronellol essential oils on the biophysical gating properties of AMPA receptors, Appl. Sci. 9 (21) (2019) 4693, doi:10.3390/app9214693.

[39] S.R. Kim, M.J. Park, M.K. Lee, S.H. Sung, E.J. Park, J. Kim, S.Y. Kim, T.H. Oh, G.J. Markelonis, Y.C. Kim, Flavonoids of inula britannica protect cultured cortical cells from necrotic cell death induced by Glutamate, Free Radic. Biol. Med. 32 (7) (2002) 596–604, doi:10.1016/s0891-5849(02)00751-7.

[40] M. Qneibi, N. Jaradat, M. Hawash, A. Olgac, N. Emwas, Ortho versus Meta Chlorophenyl-2,3-Benzodiazepine Analogues; synthesis, molecular modeling, and biological activity as AMPAR antagonists, ACS Omega 5 (7) (2020) 3588–3595, doi:10.1021/acsomega.9b04000.